Nondestructive Characterisation of the Effect of Asphalt Mixture Compaction on Aggregate Orientation and Segregation Using X-ray Computed Tomography

Norhidayah A. Hassan[1+], Gordon D. Airey[1], Rawid Khan[2] and Andrew C. Collop[1]

Abstract: The orientation and distribution of aggregates in asphalt mixtures have significant influence on asphalt mixture performance. This study investigates the effect of different compaction methods on the aggregate structure. Three laboratory compaction methods; namely gyratory, vibratory and slab roller compaction are used to compact gap graded asphalt mixture specimens. All specimens are scanned using X-ray computed tomography (CT) and the characteristics of the images are analysed. Using the image analysis technique, the aggregate particles ($\geq$ 2 mm) are separated from the mixture and the orientation and distribution in the compacted specimen are characterised. It was found that aggregates near the edge of a specimen tend to form circumferential alignment while the aggregates near the centre of the specimen are randomly oriented. Aggregate gradations show that coarse particles are mostly concentrated at the bottom compared to the top of a specimen.

Key words: Asphalt mixture; Image analysis technique; Image processing; X-ray computed tomography.

Introduction

The properties of asphalt mixtures are well established as highly dependent on microstructure including air voids, aggregates and mastic. The ability to characterise the microstructural properties is essential to understand the behaviour or macroscopic response of the material. In recent years, studies have been done to quantify the microstructure of asphalt mixtures using imaging technology, namely X-ray Computed Tomography (CT), and image analysis techniques. Based on previous research, it seems that the application of X-ray CT in characterising the aggregate structure in an asphalt mixture is limited compared to its application for air voids characterisation [1-2]. One of the main challenges in processing and analysing the X-ray CT images is the segmentation of the aggregate area. The difficulty associated with the X-ray CT images is the fact that aggregates have different grey levels, dependent on the composition of their minerals.

An alternative method to X-ray CT imaging involves two-dimensional analysis conducted on images of cut sections of a specimen where the images are captured using a digital camera. It is worth noting that images from the digital camera have less variation of grey intensity compared to X-ray CT images as grey intensity depends on the original colour of the aggregates. Researchers have used this method to study the aggregate structure and concluded that construction operations, particularly compaction method and compaction efforts, can contribute to significant changes in aggregates structure [2-7]. However, this approach is destructive and ineffective in dealing with damaged specimens. In addition it only provides an approximation to roughly estimate the actual three-dimensional distribution from two or three images of cut sections.

The disadvantage of using the digital camera approach could be rectified by capturing the image using X-ray CT. The X-ray CT approach allows the aggregate structure to be accurately and non-destructively characterised at the microstructure level. With an extensive image analysis technique carried out on the X-ray image, it is possible to minimise the error in defining the aggregate area. In this paper, the gap graded aggregates structure of a UK specified Hot Rolled Asphalt (HRA) mixture was quantitatively investigated in terms of aggregate orientation and segregation. The effect of different compaction methods was examined based on analysis carried out on the X-ray CT images. The results from the non-destructive analysis were then compared to previous research which demonstrated that compaction method has a significant effect on the aggregate structure resulting in specimens with identical volumetric properties showing various mechanical performances [6-7].

Mixture Design

The specimens were prepared to achieve the target composition for HRA (60/20) that conforms to BS 954-1:2005 (Table 1) which contains 60 percent coarse aggregate with a maximum aggregate size of 20 mm. This mixture type was employed to provide the gaps between the aggregate sizes which make it easier to identify (by scanning) the different material phases inside the specimen. Three laboratory compaction methods were used to investigate the effect of compaction methods on the aggregate structure. Two replicates were prepared for each type to achieve the same target air voids content of 5%. The details for the compaction methods are as follows:

- Gyratory (BS EN 12697-31:2007): applied pressure, 0.6 MPa, gyratory angle, 1.25° with 30 gyrations per minute.
- Vibratory (BS EN 12697-32:2003): vibrating Kango hammer

---

[1] Nottingham Transportation Engineering Centre, University of Nottingham, University Park, Nottingham NG7 2RD, UK.
[2] Department of Civil Engineering, University of Engineering and Technology Peshawar, Pakistan.
+ Corresponding Author: E-mail evxna5@nottingham.ac.uk

Table 1. Aggregates Gradation for Sieve Analysis.

Sieve Size (mm)	Percent Passing (%)
31.5	100
20	99.1
14	54.4
2	37.3
0.5	20.1
0.25	13.9
0.063	6.3

(a)

Aggregates with different mineral compositions

Mastic

(b)

Fig. 1. (a) Configuration of Scanned Specimen (b) X-ray Image of HRA.

was applied to both faces of the specimen to achieve the target height for the specified density.
- Slab roller (BS EN 12697-33:2003): smooth steel roller compactor was used with applied pressure, 0.1 MPa.

Gyratory and vibratory cylindrical specimens were produced with a diameter of 100 mm and height of 100 mm. For slab, four cylindrical specimens with the same dimension were cored from 300 mm×300 mm×100 mm slabs. Bulk density of the specimens was determined using sealed specimens (BS EN 12697-6:2003). The material properties and the mixing and compaction temperatures used for this study are as follows:
- Aggregate type   Granite
- Aggregate bulk specific gravity   2.78
- Bitumen specific gravity   1.03
- Bitumen grade   100/150 pen
- Bitumen content   5.7%
- Bitumen and aggregate pre-heated temperature   145℃
- Mixing temperature   145 ± 5℃
- Compaction temperature   135± 5℃
- Maximum and target density (kg/m^3)   2566 kg/m^3 & 2438 kg/m^3
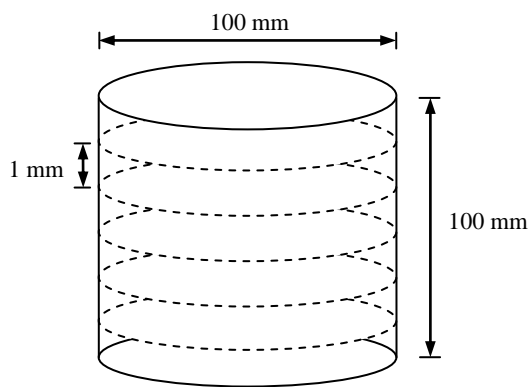
Image Analysis Study

The specimens were non-destructively scanned using an X-ray CT machine with a 350 kV source to generate a map representing the density at every point in the microstructure with the resolution of approximately 0.083 mm/pixel. Horizontal two dimensional image slices were captured relative to the specimen's height from bottom to top at every 1 mm interval. The images were saved in TIFF format as 8 bit images which consist of 256 levels of grey intensity (0 to 255). The geometry of the cylindrical specimen and an example of a captured X-ray CT image are shown in Fig. 1. Two imaging software packages, ImageJ and Image-Pro Plus, were used to process and analyse the images.
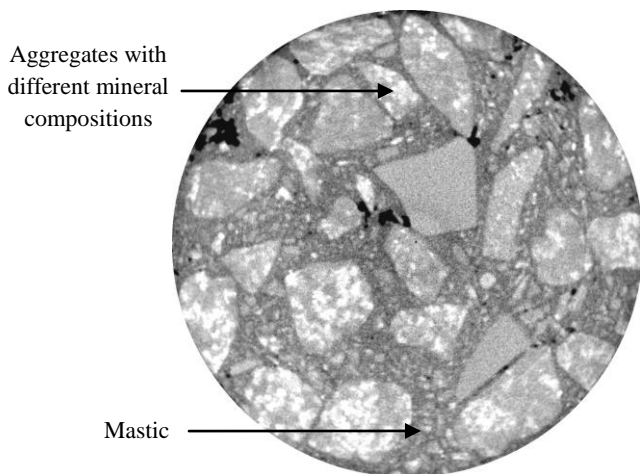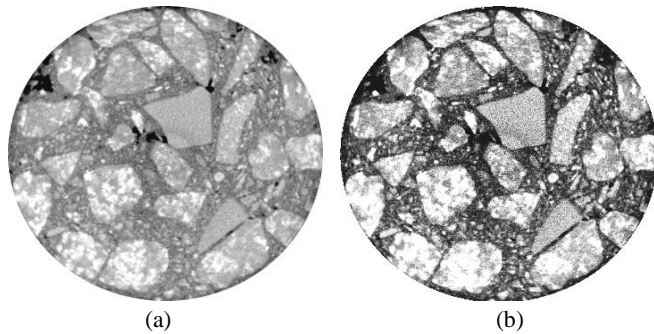
Image Processing Procedures

The internal volumetric structure of an asphalt mixture consists of three main phases; aggregates, air voids and mastic. The variation in grey intensity of the X-ray image depends on the density of each material in the composite. Brighter regions correspond to dense objects, such as aggregates, and dark regions correspond to low density objects, such as air voids. For aggregate characterisation, the image of aggregate particles must be clearly defined through the image processing. A 'thresholding technique' was adopted as a segmentation tool to distinguish the constituents of the microstructure. The aggregate particles were identified by choosing the right threshold values which significantly relies on the image quality. The automatic selection of optimum threshold remains a challenge in image segmentation. The main difficulties are due to the following facts:

i. Images of aggregates have different grey scales which depend on their mineral compositions. The grey scale cannot be uniform where the variations in dark and light grey appear within the aggregate cross section (Fig. 1(b)). This makes it difficult to choose a specific threshold value to isolate aggregates from other materials.

ii. Two or more fine aggregates that touch each other can be recognised as one large aggregate by the imaging software.

iii. The mastic surrounding the aggregate cross-section consists of bitumen and fine particles. As a result, this combination produces different grey levels for the mastic. Small portions of bitumen or fines which are not uniformly blended will increase the variation in grey scale.

To overcome these difficulties, different procedures for image processing were investigated and numerous repeat scans were undertaken to obtain better images. Finally, using the imaging software packages, the following procedures were proposed for aggregate segmentation:

(a)   (b)

Fig. 2. Comparison of X-ray Image (a) before and (b) after Equalisation

i. Preliminary treatments are necessary prior to segmentation because the quality of the original image can be variable. The brightness and contrast of images were adjusted to enhance the clarity of aggregate against the surrounding mastic using 'pixel intensity equalisation'. This transformation produces an image with the highest possible contrast and preserves almost all the details of the original image. The images before and after intensity correction are shown in Fig. 2.

ii. Threshold and segmentation tools were used to extract aggregates from the background image. Image profiles were used to clarify the aggregates area from the other material phases (mastic and air voids) by selecting the range of threshold values which relate to the grey level of the aggregate (Fig. 3(a-b)). Fig. 3(b) shows an image profile of grey level range for the 100 mm yellow line drawn in Fig. 3(a). A range of potential threshold values was then selected which matched the total area of aggregates from the design gradation curve with that obtained from the image analysis. It must be noted that, a number of image profiles were analysed for the entire image slices. From the image profiles, the range of threshold values for aggregate particles is selected between 100 and 200 grey level (shaded in blue). For mastic, the grey level is shaded in purple. The judgement is based on the fact that the percent of the selected total aggregates area is comparable to the total percentage of aggregates in the specimen. The threshold values were adjusted to isolate the aggregate particles from other material phases (Fig. 3(c-d)).
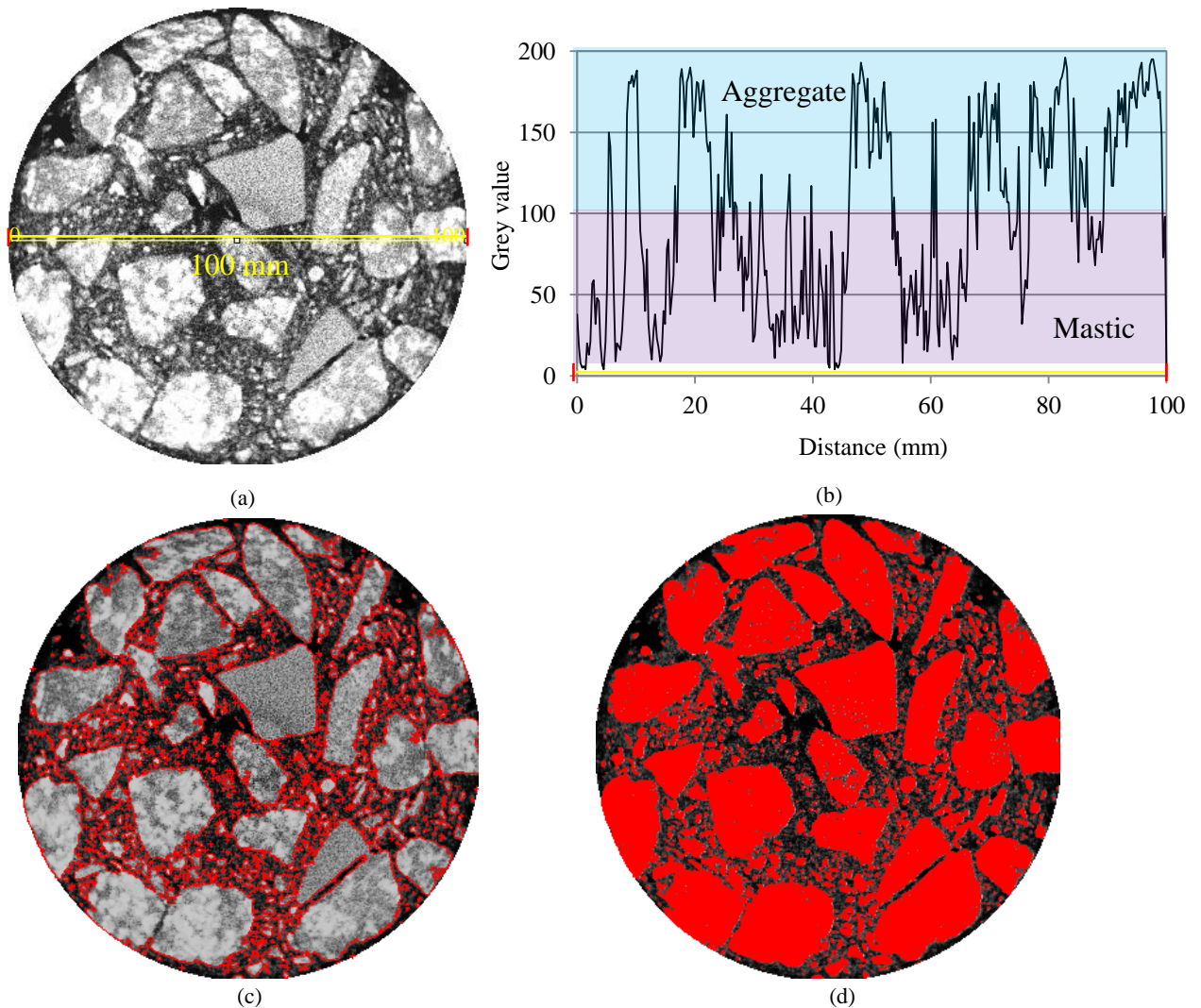

(a)   (b)

(c)   (d)

Fig. 3. Thresholding Technique (a) Image after Equalisation (b) Image Profile for the Yellow Line (100 mm) in (a), and Thresholded Images with (c) 'Outline' and (d) 'Fill' on Selected Area

iii. Based on the thresholded image, the boundary between two aggregates, in contact with each other, was unrecognised because the automatic boundary recognition tool was unable to satisfactorily detect the boundary's pixels due to the small difference in grey levels. Therefore two aggregates in contact were detected as one large aggregate (Fig. 4(a)). Also, different mineral compositions in aggregate tend to create different grey levels within the image of aggregate particles after x-ray scanning. This has resulted in uneven area or "holes" within the aggregate cross-section after thresholding (Fig. 4(b)). Therefore, the image was further enhanced using image processing tools (edge detection, holes removal, merging and splitting). These tools were used to outline the boundaries and fill the holes within the aggregate cross-sections. For example, with the 'splitting tool' specifically set to the watershed transformation, the image of two aggregates in contact was divided into regions and their boundaries were then determined as shown in Fig. 4(c). The 'holes removal tool' fills the region within the image boundary (Fig. 4(d)). It is important to note that these processes have to be performed with great care to avoid unnecessary over segmentation or the loss of any information prior to binarisation.

iv. Once all the aggregates were isolated, the posterise-threshold tool was applied and the image was transformed to a binary image (black and white). The black represents the aggregates and the white constitutes the background. Posterisation of an image entails conversion of a continuous gradation of tone to several regions of fewer tones with abrupt changes from one tone to another. To validate the selected area of interest, an 'overlapping technique' was applied by superposing the original grey scale image with the binary result (Fig. 5).

v. Another tool called 'Pseudo-colour' applies an artificial colouring on an image which can reveal textures and qualities within the image that may not have been apparent in the original grey scale. This technique can be used to reveal an image's hidden texture by assigning colours to different grey scale values which maps to a full colour range. It is based on the knowledge that the grey levels (intensities) in the image represent the linear absorption coefficients of the elements in the materials and assigns pixels with similar grey levels and hence similar absorption coefficients to a colour. Since each colour in the Pseudo-colour represents a range of grey levels and this corresponds to material phases, its microstructure can be determined [8]. The equalisation tool was then used to enhance the pixel contrast and the particles boundary (Fig. 6).

The steps listed above were applied independently or in combination, depending on the image quality as there is no universal method for image processing. Therefore it should be noted that this is a general framework of image processing operations proposed for this particular asphalt mixture X-ray CT image.

These operations were validated by comparing the aggregate gradation from X-ray CT images to the mechanical sieve analysis gradation. The aggregate gradation from image slices was calculated based on the percentage of the areas of different aggregate sizes (≥ 2 mm) within the image slices. It was highlighted in the previous study that the sieve gradation was governed by the lengths of the intermediate and minor axes of the particles [3]. Therefore, image
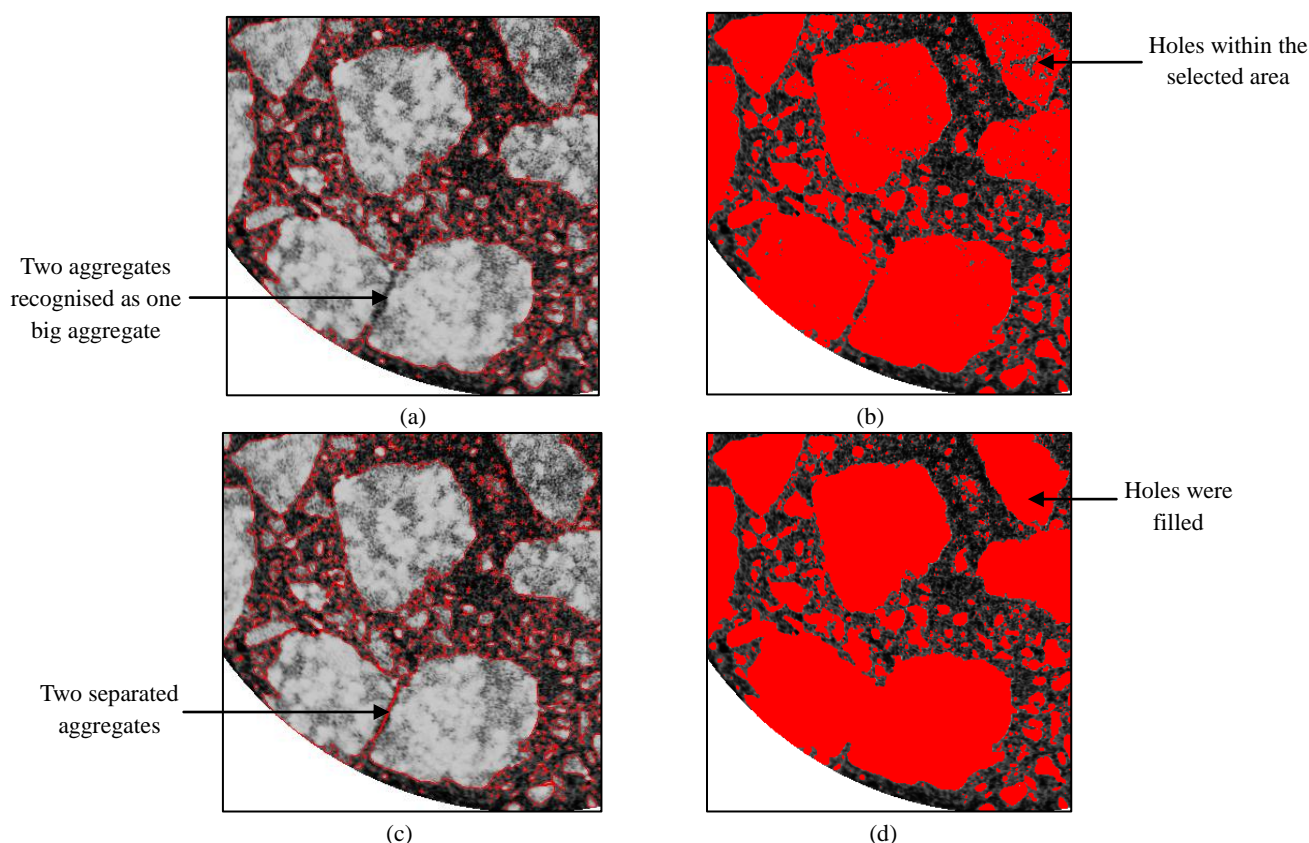

Fig. 4. Aggregates Image with (a) Outlined before Splitting (b) Filled Area (c) Outlined after Splitting (d) Filled Area after Holes Removal.
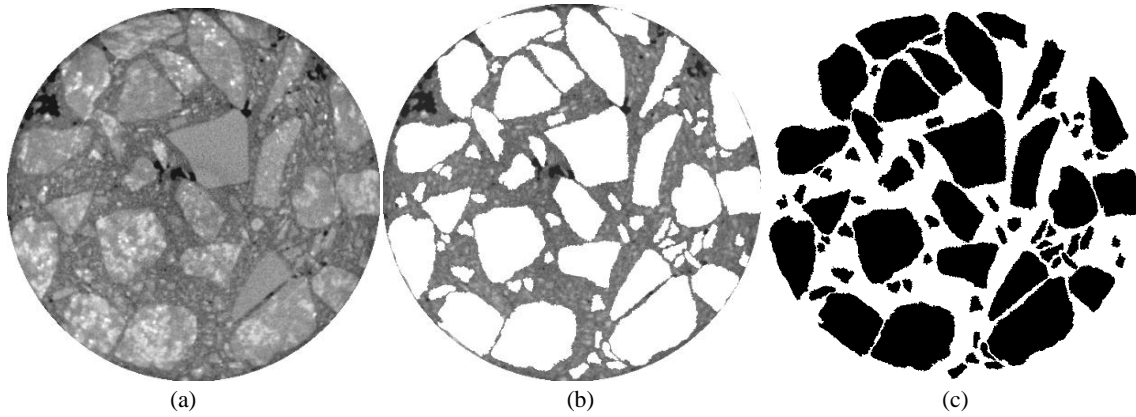
(a)   (b)   (c)

Fig. 5. Overlapping Technique for Aggregates (a) Original Greyscale Image (b) Overlapping Image (c) Binary Image after Thresholding
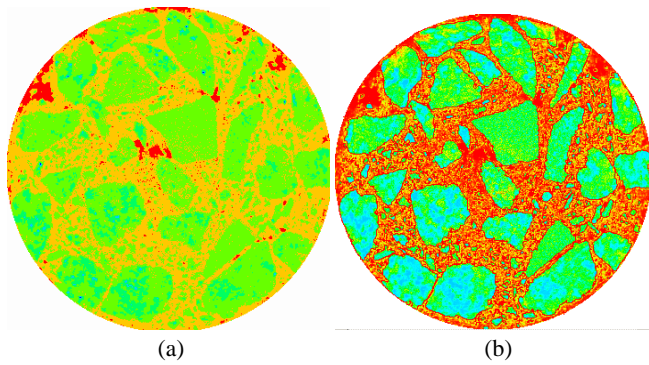

(a)   (b)

Fig. 6. Images after Applying Pseudo-colour Transformation (a) Pseudo-colour for Original X-ray Image (b) after Equalisation.

gradations were calculated based on three dimensions of the aggregate cross-sections (feret maximum diameter, F_{max}, feret minimum diameter, F_{min}, and diameter of equivalent projection area of a circle, D_{EQPC}) as the cut sections were possibly governed by the minor, intermediate and major axis lengths of the particle. F_{max} and F_{min} can be defined as the maximum and minimum distance respectively between any two pixels of the aggregate boundary. D_{EQPC} is widely used for the evaluation of particles sizes from the projection area of a non-spherical particle. It can be defined as the diameter of a circular aggregate that has the same area, A, as the aggregate being measured which can be calculated using Eq. (1).

$$D_{EQPC} = 2 \times \sqrt{A/\pi} \tag{1}$$

These three image gradations were then compared to laboratory sieve gradation for different compaction methods (Fig. 7). It can be observed that the area gradations calculated from the image analysis lie close to the laboratory measured gradation indicating their comparability. Area gradation for dimension, D_{EQPC}, was the closest to the sieve gradation and therefore was selected for further image analysis of aggregate characterisation.

Image Analysis Procedures for Characterisation

The image analysis procedures presented in this section provide quantifying parameters of the internal structure of asphalt mixtures in terms of aggregate segregation and orientation. Aggregate was characterised by considering aggregates with the size approximately
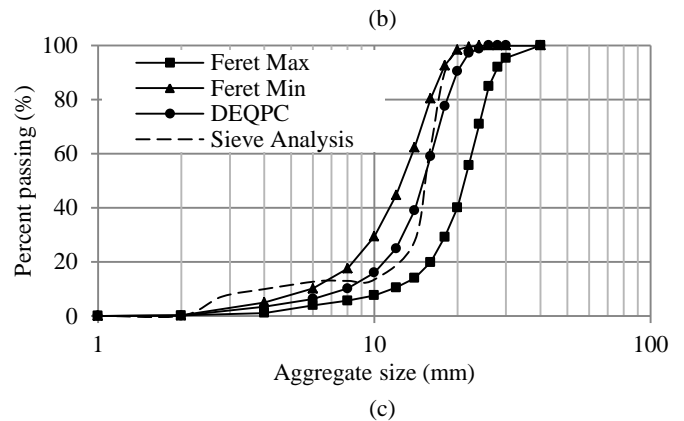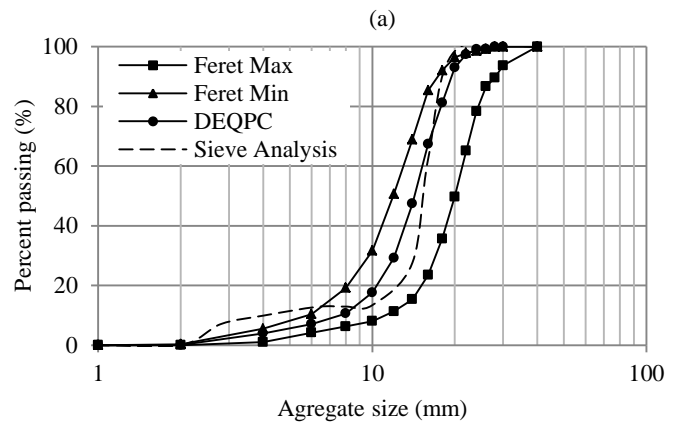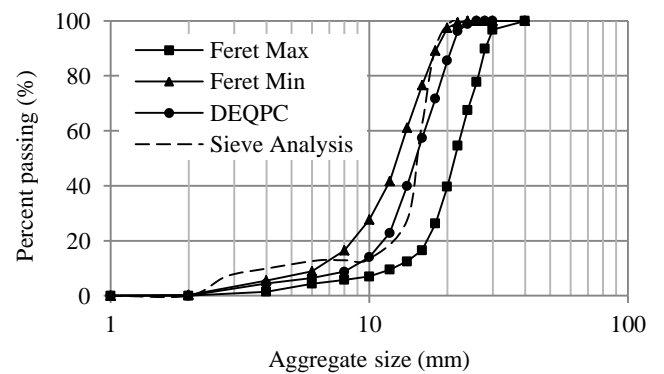

(a)

(b)

(c)

Fig. 7. Comparison of Image Gradations for Different Compaction Methods (a) Gyratory (b) Vibratory (c) Slab Roller to the Mechanical Sieve Analysis of Aggregate.

≥ 2 mm. Fine aggregate (< 2 mm) was considered to be part of the mastic because of the difficulty in identifying the small individual aggregate particles due to computational constraints. However, since this is a gap graded asphalt mixture, studying the distribution of large aggregates will adequately describe the aggregate structure in the specimen. Once the aggregate particles were identified and isolated from the background, image analysis procedures were conducted to extract valuable information on their size, location and shape properties. Two dimensional image data, including the basic parameters of aggregate cross-section, were generated using the imaging software as follows:

i. Particle area (mm^2) - area selection in square pixels with calibrated units in millimetres.
ii. Centroid - the centre point of the object in (x, y) coordinate system.
iii. Feret angle ($\theta_f°$) - angle between the F_{max} to the x-axis of the particle.
iv. Diameter of equivalent projection area of a circle, D_{EQPC}.

Aggregate Segregation

Aggregate segregation was quantified by dividing the specimen into different sections, as illustrated in Fig. 8. These sections were considered for evaluating the segregation in vertical and radial directions. The number, area and dimensions of aggregates were calculated for each section. The area gradations as a function of the dimensions were then plotted and compared between different sections. The percent ratio of average aggregate area between sections, S_L [2] was calculated using Eq. (2).

$$S_L = \left(\frac{\text{Average of aggregate area in the outer or top region}}{\text{Average of aggregate area in the inner or bottom region}} - 1 \right) \times 100 \quad (2)$$

S_L with zero value indicates no segregation occurs, while a positive value indicates coarser aggregates are distributed in the outer or top region. When the value is negative, it means that more coarse aggregates are distributed in the inner or bottom region.

Aggregate Orientation

The particle orientation was investigated in radial and circumferential alignment relative to the core centre. It was measured by the angle between its maximum feret diameter, F_{max}, and the radial line (line from core centre to aggregate centroid). Fig. 9 shows the horizontal plane of a specimen section indicating the angle of particle orientation, θ_o. The average angle of particle orientation, $\bar{\theta}_o$, was then calculated using Eq. (3) where N

Radial direction
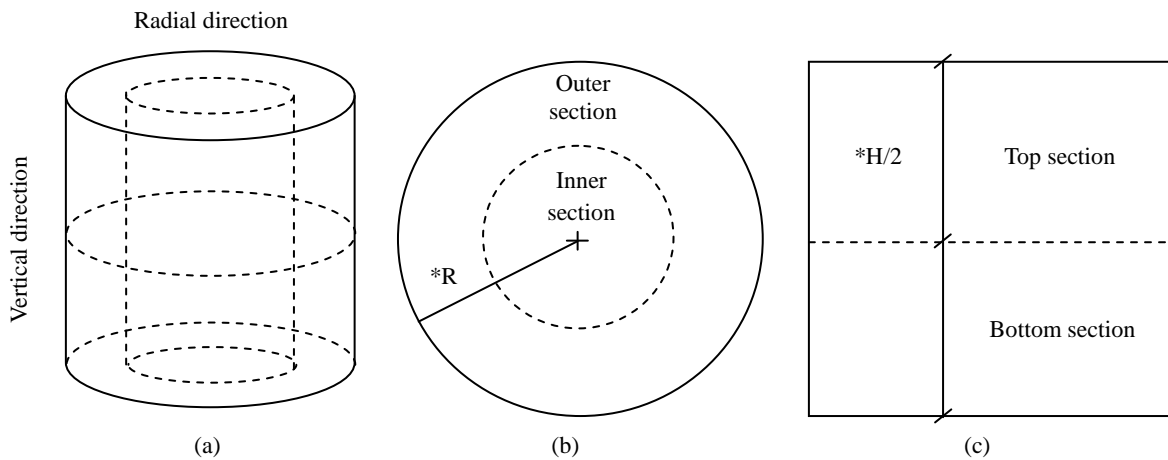
*R = radius, H = height, Volume inner = Volume outer
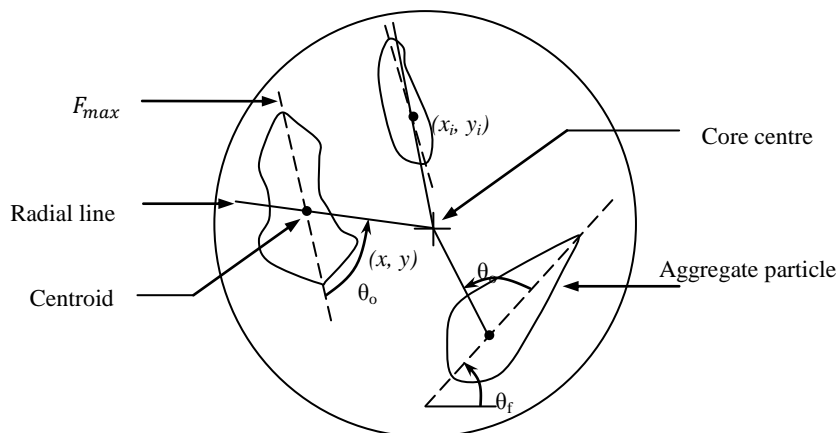**Fig. 8.** Illustration of Sections (a) Cylindrical Specimen (b) Radial and (c) Vertical Segregation.

Fig. 9. Aggregate Particles Orientation Relative to the Centre of Cross Section.

Table 2. S_L Values for Aggregate Vertical and Radial Segregations.

Specimen	Vertical segregation			Radial segregation		
	Average area (mm^2)		S_L	Average area (mm^2)		S_L
	Top	Bottom		Outer	Inner	
Gyratory	65.3	79.6	-18	62.2	55.5	12
Vibratory	63.4	78.5	-19	59.4	55.6	6.9
Slab	70.9	85.5	-17	56.4	69.3	-18.4

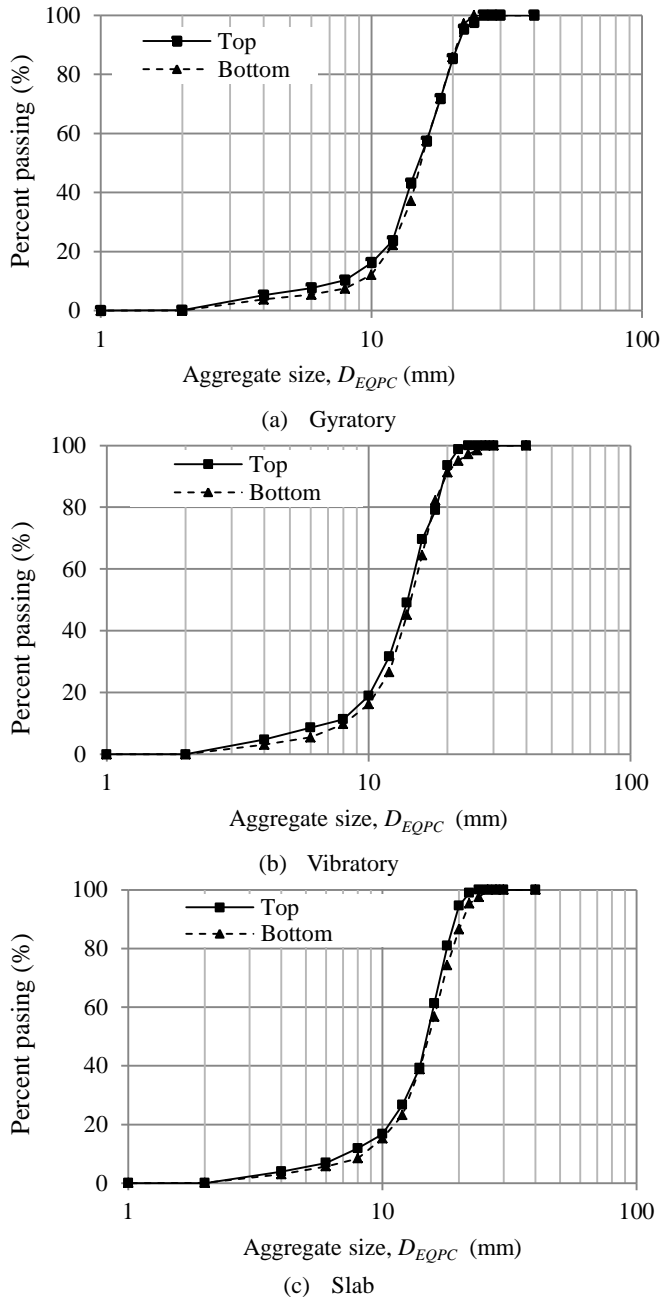(a) Gyratory

(b) Vibratory

(c) Slab

Fig. 10. Aggregate Vertical Segregation as a Function of Aggregate Size, D_{EQPC} for Gyratory, Vibratory and Slab Specimens.

=number of aggregates on the image [7].

$$\bar{\theta}_o = \frac{\sum \theta_o}{N} \tag{3}$$

$\bar{\theta}_o$ varies from 0° to 90° where particles with $\bar{\theta}_o = 0°$ were

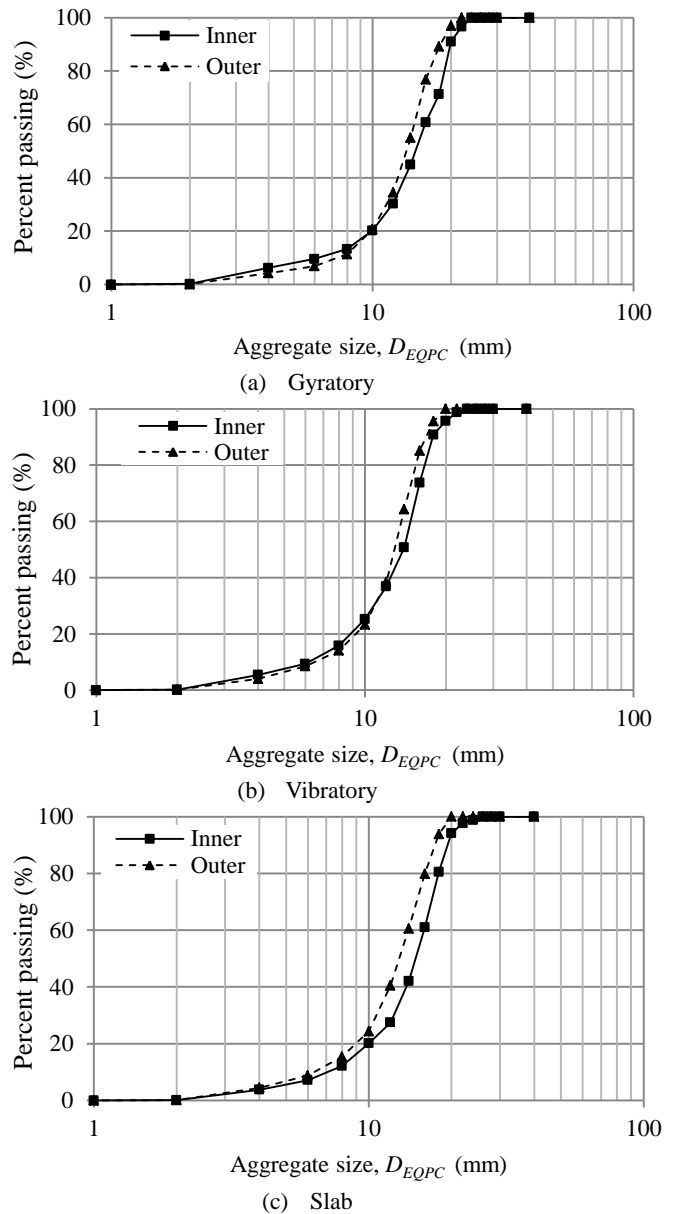
(a) Gyratory

(b) Vibratory

(c) Slab

Fig. 11. Aggregate Radial Segregation as a Function of Aggregate Size, D_{EQPC} for Gyratory, Vibratory and Slab Specimens.

considered to be oriented in the radial direction and $\bar{\theta}_o = 90°$ considered to be oriented in the circumferential direction. Random distribution was considered for the average value of $\bar{\theta}_o = 45°$. The average orientation angles were calculated throughout (from top to bottom) specimens and also compared between the inner and outer sections.

Results and Discussion

Aggregate Segregation

Table 2 summarises the percent ratio of average aggregate areas between sections, S_L. Detailed aggregate distributions in vertical and radial directions are presented in Figs. 10 and 11. As shown in the Figures, there is a minor segregation in both vertical and radial directions for all specimens. In the vertical direction, there is a slight
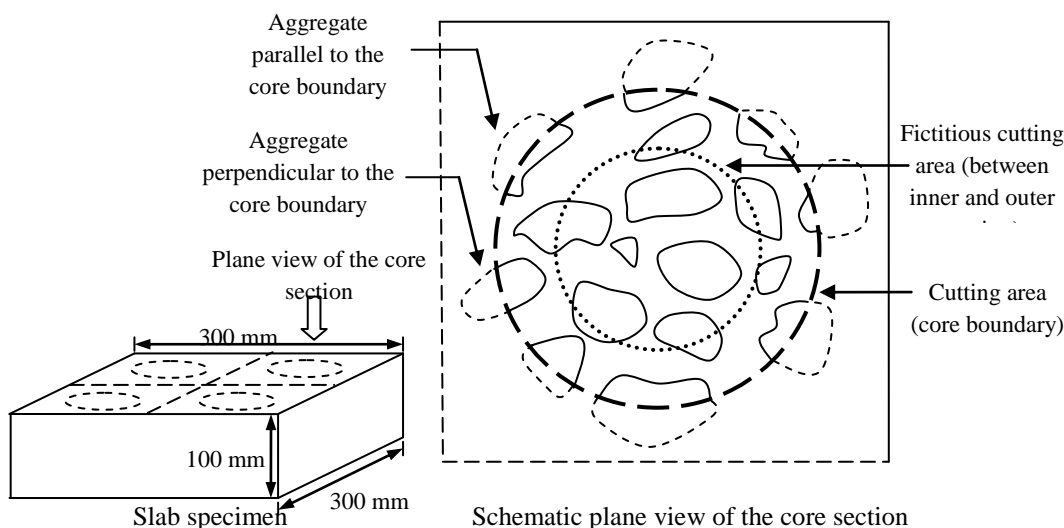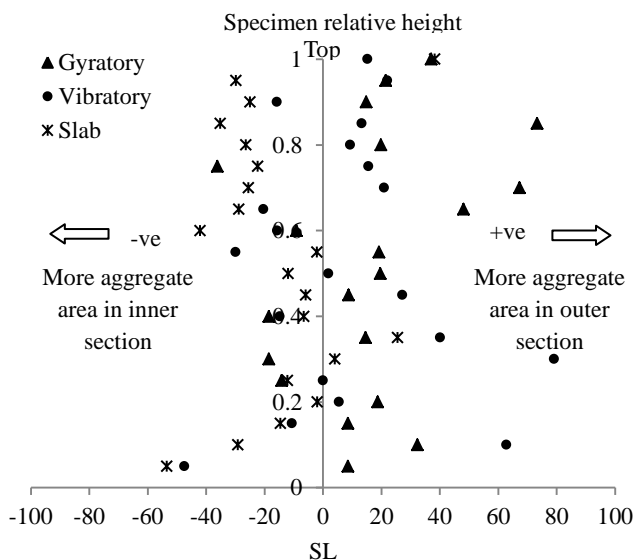
Fig. 12. Coring Section from a Slab.

Fig. 13. S_L Values of Radial Segregation Throughout Specimens.

Table 3. Average Orientation Angle of Aggregates, $\overline{\theta}_o$

Specimen	Throughout Specimen	Radial Direction	
		Outer	Inner
Gyratory	53.3°	56.5°	49.9°
Vibratory	51.1°	55.6°	46.4°
Slab	53.2°	59.4°	46.2°

vibratory specimens show slightly coarser gradation in the inner section compared to outer section. However, positive S_L values for gyratory and vibratory specimens describe higher aggregate area in the outer section than inner section with less aggregates separation for vibratory specimens (Table 2). This explains by the gradation curves where the higher aggregate area is contributed by the aggregate size less than 10 mm. For slab specimens, both gradation curve and the S_L value confirm more coarse aggregates in the inner section possibly due to the coring process (Fig. 12). In this study, a slab was produced with dimensions of 300 mm × 300 mm × 100 mm in height. Four cylindrical cores with diameter 100 mm were taken out from the slab. The cutting process near the outer section tends to reduce the size of aggregate in the outermost area. As a result, finer gradation is found in the outer section. Fig. 13 exhibits the detailed distribution of S_L values between the inner and outer section within the specimens.

Aggregate Orientation

Table 3 summarises the average aggregate orientation angle throughout the specimens. The average orientation angles for all specimens are calculated around 50° which indicates that the aggregates form an approximately random distribution from top to bottom. To compare the effect of mould confinement and coring process on aggregate orientation near the specimen's circumference, the specimen cross-section is divided into inner and outer sections. The result shows that higher average orientation angles are obtained in the outer section compare to inner which means aggregates near the mould circumference tend to form circumferential alignment. Aggregates in the inner section form a random orientation with the angle close to 45°.

Fig. 14 shows the detailed distribution of orientation angle, θ_o for aggregate particles in an image slice at the middle section of a vibratory specimen. It must be noted that in this study 100 image slices have been analysed for each specimen. There is considerable scatter in the typical plotted graph. However, the gradient of the linear graph describes the general trend of orientation angles as a function of aggregate area. The average gradient of the distribution
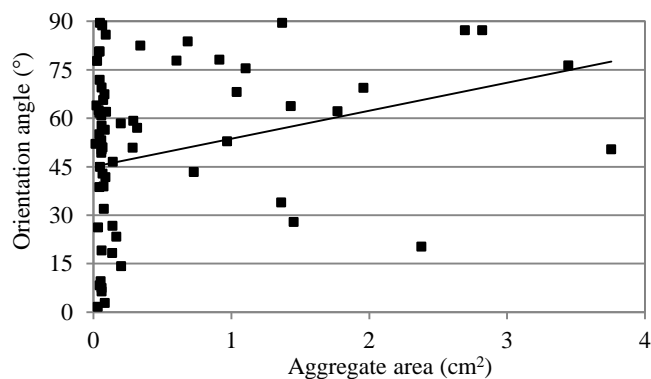
difference in the aggregate gradations which indicate more coarse aggregates present at the bottom than top section with the S_L values around -20. This separation could possibly occur when transferring the loose mixture into the mould upon compaction. Coarse aggregates tend to settle first due to gravity, whereas small aggregates stick together and are likely to accumulate at the top. For vibratory specimens, when the vibration was applied during compaction, coarser particles tend to move downwards and smaller particles tend to move towards the surface.

In the radial direction, the gradation curves for the gyratory and

Fig. 14. Orientation Angle, θ_o as a Function of Aggregates Area for the Middle Section of a Vibratory Specimen.

Table 4. Average Gradient (°/cm²) of Particle Orientation Angle versus Particle Area.

Specimen	Throughout Specimen	Radial Direction	
		Outer	Inner
Gyratory	4.68	8.24	1.76
Vibratory	4.4	11.24	-0.12
Slab	4.41	7.6	2.09

is then calculated based on 100 slices of scanned images throughout the specimen as presented in Table 4. Positive average gradient values throughout (from top to bottom) for all specimens show a general trend towards circumferential alignment with an increase in particle size. In the radial direction, this pattern is more pronounced in the outer section compare to the inner section. Therefore, it is assumed that higher aggregate orientation is mainly contributed by the influence of mould confinement. This could lead to larger aggregate sizes having a preferred orientation towards the mould circumference as they are affected by the gyratory and vibratory motion during compaction. For slab specimens, the increase towards circumferential alignment is possibly dominated by the edge cutting of aggregate particles during the coring process.

Conclusions

From this study, the following conclusions can be drawn:
- The proposed image processing procedures are able to distinguish aggregate particles from the background image for analysis purposes.
- Gyratory and slab roller compaction produce almost identical gradations and slightly coarser than vibratory compacted specimens. This may be explained by aggregate breaking due to the vibration compared to the gentle rolling by the action of gyratory and slab roller compaction.
- Segregation analysis shows that all specimens are found vertically comparable with slightly coarser gradation at the bottom than top section. In the radial direction, more coarse aggregates are observed in the inner section compared to outer section for all specimens. This is more obvious for slab specimen which is possibly due to the coring work.
- The average orientation angles for all specimens are found to be comparable with the value of approximately 50°. This indicates

that the aggregates are almost randomly oriented throughout specimens from top to bottom. However, higher average orientation angles are obtained in the outer section compared to inner section. This shows that aggregates in the outer section tend to form circumferential alignment while aggregates in the inner section form an approximately a random distribution.

Acknowledgements

References

1. Masad, E., Jandhyala, V. K., Dasgupta, N., Somadevan, N. and Shashidhar, N. (2002); "Characterization of Air Void Distribution in Asphalt Mixes using X-ray Computed Tomography", *Journal of Materials in Civil Engineering*, Vol. 14(2), pp 122-129.
2. Tashman, L., Masad, E., Peterson, B. and Saleh, H. (2001); "Internal Structure Analysis of Asphalt Mixes to Improve the Simulation of Superpave Gyratory Compaction to Field Conditions", *Journal of the Association of Asphalt Paving Technologists*, Vol. 70, pp 605-645.
3. Yue, Z. Q. and Morin, I. (1996); "Digital Image Processing for Aggregate Orientation in Asphalt Concrete Mixtures", *Canadian Journal of Civil Engineering*, Vol. 23, pp 480-489.
4. Masad, E. (2004); "X-ray Computed Tomography of Aggregates and Asphalt Mixes", *Materials Evaluation Journal*, Vol. 62(7), pp 775-783.
5. Gopalakrishnan, K. And Shashidar, N. (2007); "Characterising the Aggregate Structure Variations in Asphalt Concrete during Compaction using Computer Automated Imaging Techniques", *International Journal Computer Applications in Technology*, Vol. 28(4), pp 295-303.
6. Masad, E., Muhunthan, B., Shashidhar, N. and Harman, T. (1999); "Internal Structure Characterization of Asphalt Concrete Using Image Analysis", *Journal of Computing in Civil Engineering* (Special Issue on Image Processing), Vol. 13(2), pp 88-95.
7. Tjahjadi, T. and Bowen, D. K. (1989); "The Use of Color in Image Enhancement of X-ray Microtomographs", *Journal of X-ray Science and Technology*, Vol. 1, pp 171-189.
8. Tashman, L., Masad, E., Peterson, B., and Saleh, H. (2001); "Internal Structure Analysis of Asphalt Mixes to Improve the Simulation of Superpave Gyratory Compaction to Field Conditions", *Journal of the Association of Asphalt Paving Technologists*, Vol. 70, pp 605-645.
9. Hunter, A. E., Airey, G. D. and Collop, A. C. (2004); "Aggregate Orientation and Segregation in Laboratory Compacted Asphalt Specimens", *Transportation Research Record*, No. 1891, pp 8-15.